p53 suppression partially rescues the mutant phenotype in mouse models of DiGeorge syndrome

Cinzia Caprio[a,b] and Antonio Baldini[b,c,1]

[a]Open University PhD Program, [b]Consiglio Nazionale delle Ricerche Institute of Genetics and Biophysics Adriano Buzzati Traverso, 80131 Naples, Italy; and [c]Department of Molecular Medicine and Medical Biotechnology, University of Naples Federico II, 80131 Naples, Italy

Edited by Harry C. Dietz, The Johns Hopkins University School of Medicine, Baltimore, MD, and approved July 16, 2014 (received for review January 31, 2014)

T-box 1 (*Tbx1*), a gene encoding a T-box transcription factor, is required for embryonic development in humans and mice. Half dosage of this gene in humans causes most of the features of the DiGeorge or Velocardiofacial syndrome phenotypes, including aortic arch and cardiac outflow tract abnormalities. Here we found a strong genetic interaction between *Tbx1* and transformation related protein 53 (*Trp53*). Indeed, genetic ablation of *Trp53,* or pharmacological inhibition of its protein product p53, rescues significantly the cardiovascular defects of *Tbx1* heterozygous and hypomorphic mutants. We found that the Tbx1 and p53 proteins do not interact directly but both occupy a genetic element of *Gbx2,* which is required for aortic arch and cardiac outflow tract development, and is a known genetic interactor of *Tbx1*. We found that *Gbx2* expression is down-regulated in $Tbx1^{+/-}$ embryos and is restored to normal levels in $Tbx1^{+/-}$;$Trp53^{+/-}$ embryos. In addition, we found that the genetic element that binds both Tbx1 and p53 is highly enriched in H3K27 trimethylation, and upon p53 suppression H3K27me3 levels are reduced, along with Ezh2 enrichment. This finding suggests that the rescue of *Gbx2* expression in $Tbx1^{+/-}$;$Trp53^{+/-}$ embryos is due to reduction of repressive chromatin marks. Overall our data identify unexpected genetic interactions between *Tbx1* and *Trp53* and provide a proof of principle that developmental defects associated with reduced dosage of *Tbx1* can be rescued pharmacologically.

Tbx1 and second heart field | pharyngeal arch artery development

The 22q11.2 deletion syndrome (22q11.2DS), also known as DiGeorge and Velocardiofacial syndromes are relatively frequent and are caused by a chromosomal deletion that includes *TBX1* as well as other genes. However, heterozygous mutation of *TBX1* alone recapitulates most of the disease phenotype (1–3). Many of the clinical findings are of clear embryonic origin, e.g., congenital heart disease and thymic hypo/aplasia. However, other symptoms are of a less obvious derivation, for example the complex adolescent/adult phenotype, such as the neurobehavioral phenotype (3), which could benefit from specific treatments. Therefore, we searched for strategies to rescue the T-box 1 (*Tbx1*) haploinsufficiency phenotype based upon our current understanding of disease pathogenesis. *Tbx1* supports cell proliferation and inhibits cell differentiation in the second heart field (SHF), a population of cardiac progenitor cells that migrate and populate the outflow tract and right ventricle (4, 5). The gene plays an important, suppressive role in a switch from the progenitor state of SHF cells to the differentiated state as they enter the heart (6). *Tbx1* loss of function leads to a reduced pool of cardiac progenitors in the SHF and their premature differentiation and, consequently, hypoplasia of the cardiac outflow tract (OFT). *Tbx1* mutation is associated with reduced cell proliferation in several other tissues, for example the pharyngeal endoderm and the otic epithelium (7, 8). In addition, *Tbx1* has also been implicated in the expansion of dental stem cells (9) and self-renewal of hair follicle stem cells (10). Based on this knowledge, we sought genetic strategies that could counteract the effects of reduced dosage of *Tbx1*. The transcription factor p53, which is encoded by the transformation related protein 53 (*Trp53*) gene, has prodifferentiation and antiproliferation activities in stem cells (11–13), and its loss of function facilitates reprogramming of differentiated cells (14, 15). Therefore, we asked whether *Tbx1* and *Trp53* interact during cardiovascular development. Results show that heterozygous deletion of *Trp53* or pharmacological suppression of p53 partially rescues the cardiovascular phenotype associated with reduced dosage of *Tbx1*. Surprisingly, we found that Tbx1 and p53 cooccupy chromatin segments, suggesting that they have shared targets. Indeed, we found that *Gbx2*, a gene required during cardiovascular development and known to genetically interact with *Tbx1* (16, 17), is targeted by both transcription factors. Specifically, it is down-regulated by *Tbx1* deletion, but its expression is reestablished to wild-type levels in the presence of *Trp53* deletion.

Our data reveal a previously unsuspected genetic interaction between *Tbx1* and *Trp53*, provide novel insights into the mechanisms of *Tbx1* function, and suggest a role of p53 in cardiac progenitors biology. Importantly, we have also established a proof of principle that the *Tbx1* haploinsufficiency phenotype can be rescued pharmacologically.

Results

Epistatic Genetic Interaction Between *Trp53* and *Tbx1*. We crossed $Trp53^{+/-}$ and $Tbx1^{+/-}$ mice and harvested embryos at embryonic day (E) 10.5 to test whether there is a genetic interaction between *Tbx1* and *Trp53*, and test its effects on the typical haploinsufficiency phenotype, i.e., hypoplasia or aplasia of the fourth pharyngeal arch arteries (fourth PAAs) (18–20). We analyzed a total of 56 embryos; the results are summarized in Table 1. WT and $Trp53^{+/-}$ embryos were all normal ($n = 32$), whereas $Tbx1^{+/-}$ were mostly abnormal (12 of 13 embryos or 92%). Double

Significance

The 22q11.2 deletion is the most common known genetic cause of congenital heart disease (CHD). The haploinsufficiency of *TBX1* has been identified as the cause of CHD. Using mouse models of the disease, we found that reduced dosage of p53 suppresses the *Tbx1* mutant phenotype. Tbx1 and p53 proteins coregulate the gene *Gbx2*, which is required for cardiovascular development. *Gbx2* expression is positively regulated by Tbx1, whereas suppression of p53 results in reduced levels of the repressive chromatin mark H3K27me3 at a genetic element occupied by both Tbx1 and p53. These data illustrate a mechanism by which reduced p53, by genetic or pharmacological means, can counterbalance the consequences of reduced dosage of Tbx1.

Author contributions: C.C. and A.B. designed research; C.C. performed research; C.C. and A.B. analyzed data; and A.B. wrote the paper.

The authors declare no conflict of interest.

This article is a PNAS Direct Submission.

[1]To whom correspondence should be addressed. Email: antonio.baldini@igb.cnr.it.

This article contains supporting information online at www.pnas.org/lookup/suppl/doi:10.1073/pnas.1401923111/-/DCSupplemental.

Table 1. Rescue of fourth PAA defects by genetic or pharmacological suppression of p53: Genetic experiment

Genotype (E10.5)	Normal	Fourth PAA defects
Tbx1$^{+/+}$	16	0
Tbx1$^{+/-}$	1	12 (92%)
Trp53$^{+/-}$; *Tbx1*$^{+/-}$	10	1 (9%)**
Trp53$^{+/-}$	16	0

"Normal" refers to the pattern of the PAA system. **$P = 0.00004$.

heterozygous *Trp53*$^{+/-}$;*Tbx1*$^{+/-}$ embryos, however, were mostly normal (10 out of 11 embryos, or 91%, $P = 0.00004$). Examples of ink injection data are shown on Fig. 1. We measured the diameter of "rescued" fourth PAAs of *Trp53*$^{+/-}$;*Tbx1*$^{+/-}$ embryos and found it very similar compared with that of WT embryos: 55.1 ± 16.1 μm ($n = 22$) for the WT and 61.3 ± 9.6 μm ($n = 18$) in rescued *Trp53*$^{+/-}$;*Tbx1*$^{+/-}$ embryos. Therefore, *Trp53* deletion almost completely rescues this particular phenotype. To exclude that rescue was due to a gene mutation linked to the mutant *Trp53* allele or to genetic background, we repeated the experiment using pharmacological suppression of p53 with the drug Pifithrin-α (21). Timing of drug administration to pregnant females was based on our findings that *Tbx1* is required for fourth PAA development as early as E7.5 but it is not longer required after E9.5 (22). Therefore, we injected Pifithrin-α into pregnant females at E7.5, E8.5, and E9.5 and harvested embryos at E10.5 to score the fourth PAA phenotype. Results (Table 2) showed again a significant suppression of the fourth PAA defect ($P = 0.00016$). Thus, genetic ablation as well as temporally restricted pharmacological suppression of p53 rescues the *Tbx1* haploinsufficiency phenotype.

***Trp53* Mutation Modifies the Hypomorphic but Not the Null *Tbx1* Phenotype.** Reduced p53 dosage may suppress the *Tbx1* mutant phenotype indirectly (e.g., through a compensatory mechanism that buffers the consequences of loss of *Tbx1*), or it may act more specifically by interacting with the normal transcriptional functions of Tbx1. Although these hypotheses are not mutually exclusive, if the second mechanism is significant, the Tbx1 protein must be present for the rescue to occur. Therefore, we first tested whether *Trp53* mutation can modify the intracardiac phenotype of *Tbx1*$^{-/-}$ embryos. To this end, we crossed *Tbx1*$^{+/-}$;*Trp53*$^{+/-}$ and *Tbx1*$^{+/-}$; *Trp53*$^{+/+}$ mice and harvested embryos at E18.5, when the cardiac phenotype can be fully assessed morphologically. Results, summarized in Table S1, revealed the rescue of the cardiovascular haploinsufficiency phenotype (at this stage it consists of anomalous remodeling of the great arteries and aortic arch), thus confirming that the fourth PAAs were not only rescued morphologically at E10.5, but they also underwent normal remodeling. However, *Tbx1*$^{-/-}$;*Trp53*$^{+/+}$ and *Tbx1*$^{-/-}$; *Trp53*$^{+/-}$ embryos were phenotypically indistinguishable (Table S1). Specifically, we examined, by external inspection and by histology, *Tbx1*$^{-/-}$;*Trp53*$^{+/+}$ and *Tbx1*$^{-/-}$; *Trp53*$^{+/-}$ hearts and scored the pattern of the aortic arch and connected arteries, type of VSD, the alignment of the truncus and ventricles, and the morphology of the outflow valves. We could not find any morphological difference between the two genotypes. Next, we used the hypomorphic allele *Tbx1*^{neo2}, which expresses ∼15% of the *Tbx1* mRNA compared with the WT allele (23). We crossed *Tbx1*$^{+/-}$;*Trp53*$^{+/-}$ and *Tbx1*$^{+/neo2}$;*Trp53*$^{+/+}$ mice and harvested embryos at E18.5. A tabulated summary of cardiac phenotyping data is shown in Fig. 2*A*. The external appearance of *Tbx1*$^{-/neo2}$; *Trp53*$^{+/+}$ and *Tbx1*$^{-/neo2}$;*Trp53*$^{+/-}$ embryos was indistinguishable and embryo dissection showed that both genotypes had absence or severely hypoplastic thymus. However, cardiac phenotyping revealed some important differences. For practical purposes, we assigned a phenotypic score (from 1 to 7, where 1 is morphologically normal and 7 is the most severe) to individual samples. The most remarkable result was the finding of 3 of the 18 *Tbx1*$^{-/neo2}$;*Trp53*$^{+/-}$ embryos examined (17%) showed a normally septated heart (Fig. 2 *B*–*C*', score 1), whereas all of the 17 *Tbx1*$^{-/neo2}$;*Trp53*$^{+/+}$ embryos examined had a complex septation defect (see, for example, Fig. 3 *A*, *B*, *E*, and *F*, scores from 4 to 7). In addition, 3 *Tbx1*$^{-/neo2}$;*Trp53*$^{+/-}$ embryos presented with a milder form (score 3) of double outlet right ventricle (DORV) or incomplete truncus arteriosus (TA). In these cases, the aorta or the truncus arteriosus were overriding the ventricular septum, whereas in *Tbx1*$^{-/neo2}$;*Trp53*$^{+/+}$ embryos they originated from the right ventricle (Fig. 3). This finding indicates that *Trp53* mutation improves the alignment between the outflow tract and the ventricles. Furthermore, we found a single case of isolated ventricular septal defect (VSD, score 2) among the *Tbx1*$^{-/neo2}$; *Trp53*$^{+/-}$ embryos (Fig. 3 *F*–*H*). In contrast, all of the *Tbx1*$^{-/neo2}$; *Trp53*$^{+/+}$ embryos examined presented with VSD associated with conotruncal septation defects or DORV (Fig. 2*A*).

Because the OFT phenotype of *Tbx1* mutants is associated with reduced cell proliferation in the SHF, we tested whether *Trp53* ablation increases cell proliferation in a *Tbx1*$^{-/neo2}$ background, thus providing a possible explanation of the partial rescue of the OFT phenotype. To this end, we performed double immunofluorescence staining of histological sections of *Tbx1*$^{-/neo2}$; *Trp53*$^{+/+}$ and *Tbx1*$^{-/neo2}$;*Trp53*$^{+/-}$ E9.5 embryos with anti-phosphorylated histone 3 (PH3, a mitotic marker) and anti-Isl1 (a cardiac progenitor marker) antibodies and evaluated the percentage of double positive Isl1+;PH3+ cells over the total of Isl1+ cells in the SHF area (operatively defined as the posterior pericardial wall excluding inflow and outflow proper) (Fig. S1). Results showed that 35.9% of the Isl1+ SHF cells were PH3+ in in *Tbx1*$^{-/neo2}$;*Trp53*$^{+/+}$ embryos and 62.7% in *Tbx1*$^{-/neo2}$;*Trp53*$^{+/-}$, significantly more than in *Tbx1*$^{-/neo2}$;*Trp53*$^{+/+}$ littermates (three embryos per genotype, $P = 7.4 \times 10^{-7}$). Thus, *Trp53* ablation had a significant impact on Isl1+ SHF cell proliferation in a *Tbx1* mutant background.

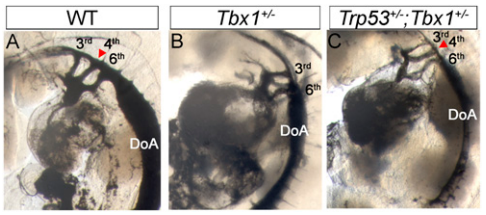

Fig. 1. *Trp53* deletion rescues the fourth PAA defects in *Tbx1*$^{+/-}$ embryos. Examples of ink injections assays for the visualization of the pharyngeal arch arteries in E10.5 embryos. (*A*) Ink-injected, WT E10.5 embryo showing the normal anatomy of the third, fourth, and sixth pharyngeal arch arteries on the left. (*B*) Ink-injected, *Tbx1*$^{+/-}$; *Trp53*$^{+/+}$ E10.5 embryo. Note the absence of the left fourth PAA. (*C*) Ink-injected, *Tbx1*$^{+/-}$; *Trp53*$^{+/-}$ E10.5 embryo. Note the presence and normal anatomy of the fourth PAA. Arrowheads indicate the fourth PAA.

Table 2. Rescue of fourth PAA defects by genetic or pharmacological suppression of p53: Treatment with Pifithrin-α

Genotype (E10.5)	Pifithrin-α	Normal	Fourth PAA defects
Tbx1$^{+/+}$	Untreated	10	0
	Treated	7	0
Tbx1$^{+/-}$	Untreated	0	10 (100%)
	Treated	14	5 (36%)*

"Normal" refers to the pattern of the PAA system. *$P = 0.00016$.

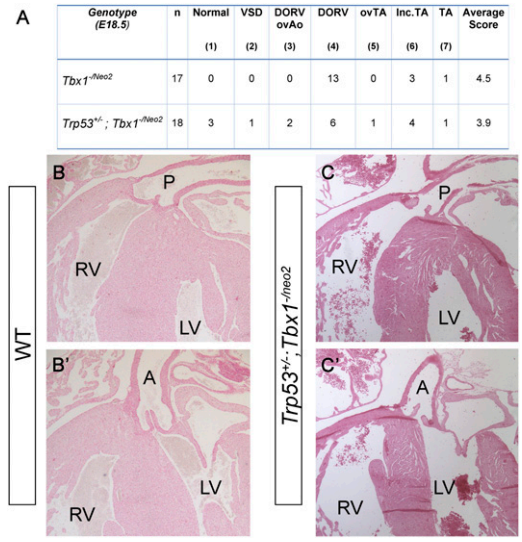

Fig. 2. *Trp53* deletion ameliorates the outflow tract phenotype in *Tbx1* hypomorphic mutants. (*A*) Tabulated summary of cardiovascular phenotype in hypomorphic mutants with and without *Trp53* deletion. n, total number of embryos examined with the genotype indicated. "Normal" refers to heart phenotype. DORV, double outlet right ventricle; ovAo, overriding aorta; ovTA, overriding of (unseptated) truncus arteriosus; TA, Truncus arteriosus communis; VSD, ventricular septal defects. The number in parentheses is the phenotypic score, an arbitrary number that indicates the severity of the phenotype, 1 being the mildest and 7 being the most severe. Histological sections of E18.5 embryo hearts showing complete rescue of ventricular and conotruncal septation. (*B* and *B*′) Two different sections of the same heart of a WT littermate of the embryo shown in *C* and *C*′. (*C* and *C*′) Two different sections of the same heart of a $Tbx1^{-/neo2};Trp53^{+/-}$ embryo. Note the normal septation of the great arteries and ventricles, similar to WT embryos. A: Aorta; LV: left ventricle; P: Pulmonary trunk; RV: right ventricle.

Tbx1 and p53 Proteins Cooccupy Chromatin Segments. To gain insights into the nature of the Tbx1–p53 interaction, we first excluded that *Trp53* is a negative regulator of *Tbx1* expression in mouse embryos (Fig. 4*A*). Next, we tested whether the two proteins interact directly. However, coimmunoprecipitation did not reveal any interaction (Fig. 4*B*). Next, we asked whether the two proteins, albeit not interacting directly, occupy the same chromatin regions. To this end, we used chromatin immunoprecipitation combined with Western blotting (ChIP–WB). Chromatin was extracted from cross-linked 5-Azacytidine/DMSO-induced P19Cl6 cells (48 h after induction), which express both *Tbx1* and *Trp53* genes (Fig. S2), fragmented to a range of 150–350 bp and immunoprecipitated using anti-Tbx1 or anti-p53 antibodies. Captured complexes were released and de-cross-linked, and proteins were subjected to Western blot analyses. Results showed that the p53 protein was present in the Tbx1-captured complexes (Fig. 4*C*) and vice versa (Fig. 4*D*). Thus, there are chromatin segments that are occupied by both Tbx1 and p53, suggesting that the two transcription factors coregulate shared targets.

The *Gbx2* Gene Is Down-Regulated in $Tbx1^{+/-}$ Embryos, Rescued by *Trp53* Mutation, and Occupied by both Transcription Factors. To identify putative shared targets, we followed a candidate gene approach. We considered three Tbx1 target genes that are known to interact with *Tbx1* during fourth PAA development: *Gbx2*, *Smad7*, and *Wnt5a* (17, 24, 25). We first tested the expression of these genes in WT, $Tbx1^{+/-}$, $Trp53^{+/-}$, and $Tbx1^{+/-}$; $Trp53^{+/-}$ E8.5 embryos using quantitative reverse transcription PCR. Results showed *Gbx2* to be the most interesting target because its expression was the most affected by heterozygous *Tbx1* deletion (Fig. 5 *A*–*C*), it was not affected by *Trp53* deletion, and, strikingly, expression returned to WT levels in $Tbx1^{+/-}$; $Trp53^{+/-}$ embryos (Fig. 5*C*). Homozygous deletion of *Gbx2* causes similar fourth PAA abnormalities to those in $Tbx1^{+/-}$ embryos, and *Gbx2* heterozygous deletion strongly enhances the *Tbx1* haploinsufficiency phenotype (17). Therefore, it is possible that at least part of the gene haploinsufficiency rescue in $Tbx1^{+/-}$; $Trp53^{+/-}$ embryos is due to rescue of *Gbx2* expression. We asked

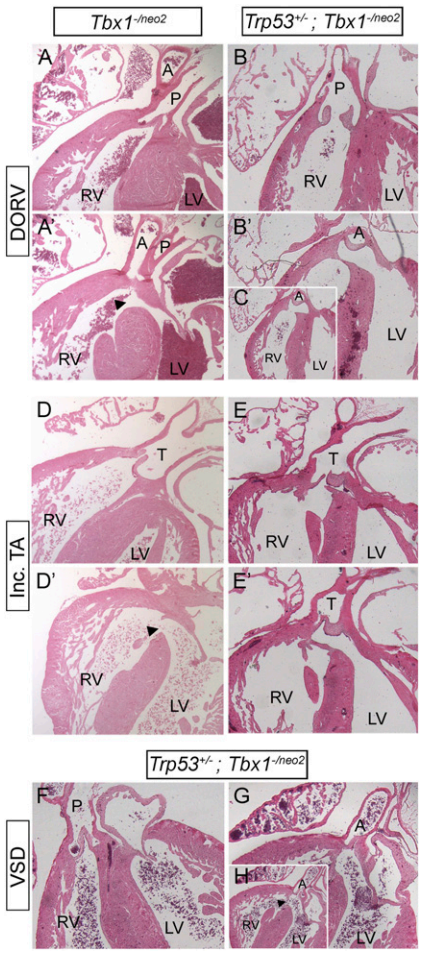

Fig. 3. *Trp53* deletion ameliorates the outflow tract phenotype in *Tbx1* hypomorphic mutants at E18.5. (*A* and *A*′) Two sections of the same heart of a $Tbx1^{-/neo2};Trp53^{+/+}$ embryo. Note that both the aorta and the pulmonary trunk originate from the right ventricle. This is an arrangement observed in all of the embryos with this genotype. (*B*, *B*′, and *C*) Three sections of the same heart of a $Tbx1^{-/neo2};Trp53^{+/-}$ embryo. The pulmonary trunk communicates with the right ventricle, whereas the aorta communicates with both ventricles, indicating a better alignment between the outflow and the heart chambers, compared with the embryo shown in *A* and *A*′. In C, the section is shown at a lower magnification to fit the panel. (*D* and *D*′) Two sections of the same heart of a $Tbx1^{-/neo2};Trp53^{+/+}$ embryo. Note that the truncus arteriosus communis (T) is positioned directly above the RV. (*E* and *E*′) Two sections of the same heart of a $Tbx1^{-/neo2};Trp53^{+/-}$ embryo. The truncus arteriosus communis communicates with both the RV and LV, above the interventricular septum. (*F*–*H*) Three sections of the same heart of a $Tbx1^{-/neo2};Trp53^{+/-}$ embryo. The pulmonary trunk is connected to the RV and the aorta to the LV. Although the latter is located above the septum, it does not directly communicate with the RV. In *H*, the section is shown at a lower magnification to fit the panel. A, aorta; DORV, double outlet right ventricle; Inc. TA, incomplete truncus arteriosus (there is truncal septation but not conal septation); LV, left ventricle; P, pulmonary trunk; RV, right ventricle; T, truncus arteriosus unseptated; VSD, ventricular septal defect. Arrowhead, interventricular communication (VSD).

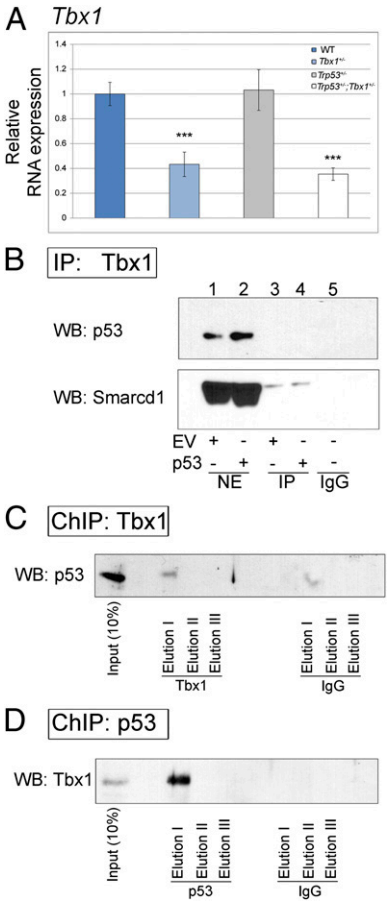

Fig. 4. Molecular analyses of *Trp53–Tbx1* interaction. (*A*) Quantitative real time PCR evaluation of *Tbx1* expression in E8.5 embryos with the genotypes indicated. Tbx1 expression is associated with heterozygous deletion, as expected, but is not affected by the presence of Trp53 deletion. ***P = 0.001. Error bars indicate SEM of five independent experiments. (*B*) Immunoprecipitation experiment using nuclear extracts from differentiated (48 h) P19Cl6 cells and an antibody anti-Tbx1. In parallel, we used also cells transfected with a *Trp53* expression vector (lanes 2 and 4). We carried out Western blotting using an antibody against p53 and Smarcd1/Baf60a (positive control). The p53 protein is not coimmunoprecipitated. (*C*) ChIP–Western blot experiment using an anti-Tbx1 antibody. The p53 protein is readily detected. (*D*) ChIP–Western blot experiment using an anti-p53 antibody. The Tbx1 protein is present in the eluate.

whether the *Gbx2* gene may be occupied by both Tbx1 and p53 proteins. To this end, we computationally searched for T-box binding elements (TBEs) and p53 binding elements (p53BEs) and found four candidates for each of these transcription factors (Fig. 6*A*). To test whether these sites are occupied, we performed ChIP of 5-Azacytidine/DMSO-induced P19Cl6 cells (48 h after induction) because, at this stage, all three endogenous genes (*Tbx1*, *Trp53*, and *Gbx2*) are expressed (Fig. S2). Quantitative ChIP using an anti-Tbx1 antibody revealed the occupation of TBE4 (Fig. 6*B*, *Left*), whereas ChIP with an anti-p53 antibody revealed occupation of p53BE3 (Fig. 6*B*, *Right*), in four independent experiments per antibody.

The gene expression data shown above suggest that p53 alone does not have a direct effect on *Gbx2* expression, but its deletion buffers the effect of the *Tbx1* deletion. Therefore, considering that p53 has been shown to interact with the Phf1 component of the Polycomb repressive complex 2 (PRC2) (26), we asked whether p53 suppression may alter the chromatin state of the *Gbx2* genetic element occupied by p53 and Tbx1. We performed qChIP with an anti-H3K27me3 antibody and found that the DNA segment is highly enriched for this histone modification, but after p53 suppression by siRNA, the levels of H3K27me3 are significantly reduced (Fig. 6*C*). Next, we asked whether H3K27me3 enrichment correlates with local enrichment of Ezh2, the histone methyltransferase that provides enzymatic activity to the PRC2 complex. To this end, we performed qChIP analysis with an anti-Ezh2 antibody and in cells with or without p53. Results revealed that this protein occupies the p53BE3 site, but its enrichment is significantly reduced following p53 knock down (Fig. 6*D*). However, Ezh2 does not coimmunoprecipitate with p53 (Fig. S3). Overall, these data suggest that p53 indirectly recruits Ezh2 to p53BE3 site, thus regulating its H3K27 methylation status.

Overall, these results indicate that *Gbx2* is regulated by both transcription factors.

Discussion

Gene haploinsufficiency is often a cause of genetic disease and indicates absence or insufficiency of genetic buffering system(s) to compensate for the loss of one copy of the gene. *Tbx1* is haploinsufficient in humans and mice and its deletion affects a number of morphogenetic and developmental processes. Phenotypic anomalies also extend into adult life, including neuropsychiatric disease, for which there is no specific treatment. Thus, discovery of strategies to buffer gene haploinsufficiency is

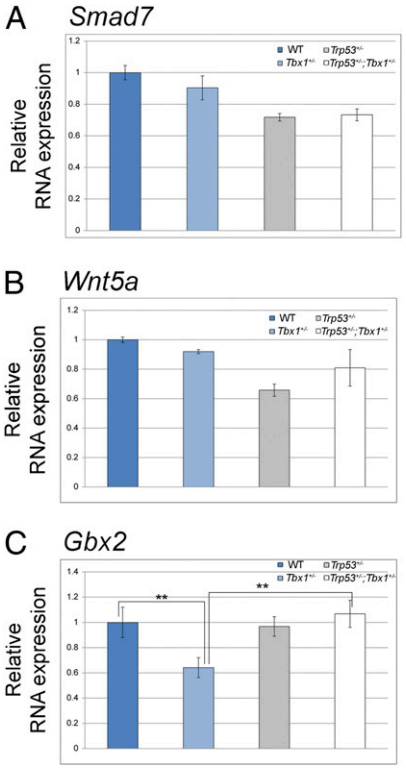

Fig. 5. Trp53 deletion rescues the *Gbx2* expression down-regulation in *Tbx1*$^{+/-}$ E8.5 embryos. (*A*) Quantitative real-time PCR (qPCR) evaluation of the *Smad7* gene expression in E8.5 embryos (two embryos per genotype). None of the variation observed are statistically significant. (*B*) qPCR evaluation of the *Wnt5a* gene expression in E8.5 embryos (two embryos per genotype). None of the variation observed are statistically significant. (*C*) qPCR evaluation of the *Gbx2* gene expression in E8.5 embryos (five embryos per genotype). The expression is significantly reduced in *Tbx1*$^{+/-}$ embryos and significantly enhanced in double heterozygous embryos. There is not significant difference between WT and double heterozygous embryos. **P = 0.004. Error bars indicate SEM of five independent experiments.

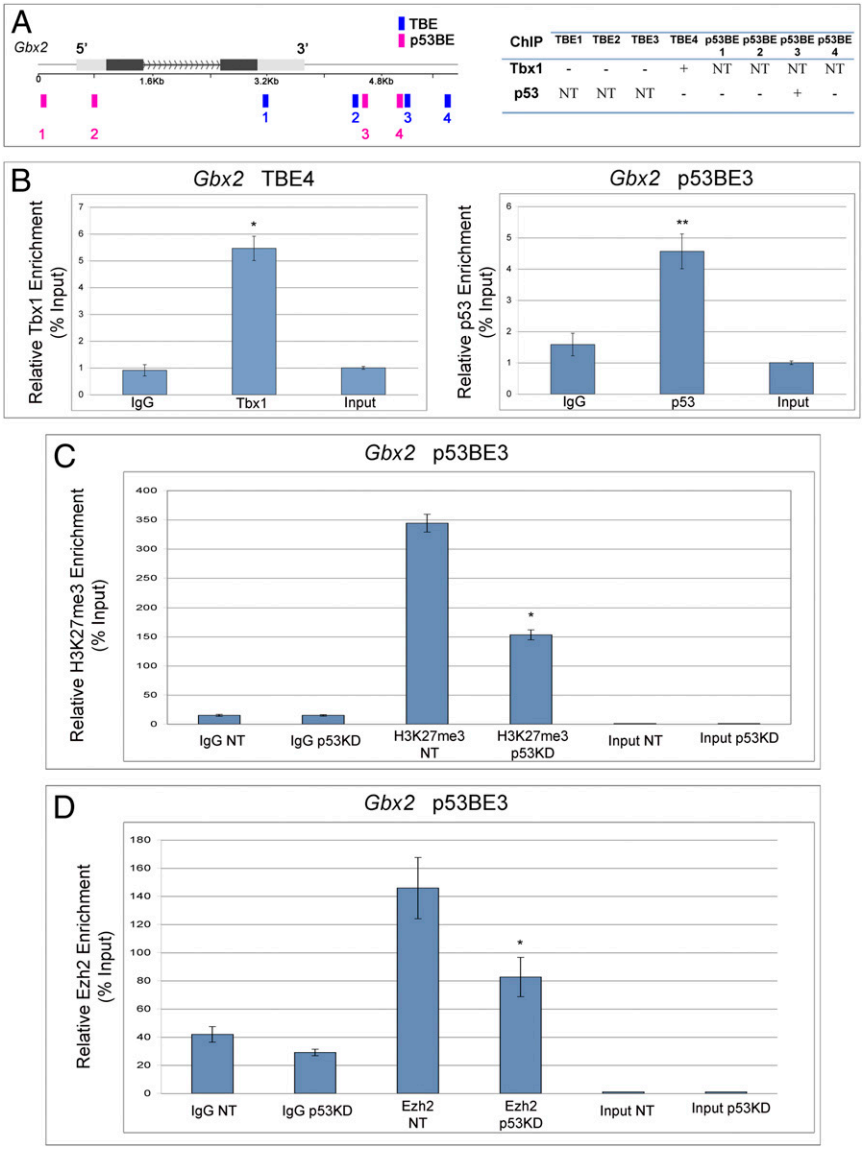

Fig. 6. p53 and *Tbx1 occupy the Gbx2 gene*. (*A*, *Left*) schematic representation of the *Gbx2* gene showing the position of computationally detected T-box (blue) and p53 (red) binding sites. (*A*, *Right*) Summary of results of ChIP experiments. +, enriched; –, not enriched; NT, not tested. The genomic coordinates (mm10) of TBE4 and p53BE3 are chr1:89925759–89925824 and chr1:89927115–89927206, respectively. (*B*) Quantitative ChIP (qChIP) results for the two enriched sites. (*Left*) ChIP using an anti-Tbx1 antibody. (*Right*) ChIP using an anti-p53 antibody. $*P = 0.04$; $**P = 0.009$. Error bars indicate mean ± SD of four independent experiments. (*C*) qChIP with an anti-H3K27me3 antibody at the p53BE3 site. The experiment was carried out from P19CL6 transfected with a control siRNA (NT) or with an anti-*p53* siRNA (p53KD). The immunoprecipitation was carried out with an anti–Trimethyl-Histone H3 (Lys27) antibody. Note that the level of H3K27me3 at the p53BE3 site is significantly lower in the *p53* knock down sample. $*P < 0.05$. Error bars indicate mean ± SD of three biological replicates. (*D*) qChIP experiment using an antibody anti-histone methyltransferase Ezh2 on the same site as in *C*. Enrichment is reduced in the samples with p53 knock down. The histogram shows the mean ± SD of three biological replicates. $*P < 0.05$.

not only important from a biological point of view, but it is also important for the development of future treatments.

In this work, we followed a rationale that was based on the contrasting effects of Tbx1 and p53 on cell differentiation and proliferation to devise a genetic and pharmacological rescue strategy. We found that *Trp53* heterozygous deletion was effective in rescuing the *Tbx1* haploinsufficient phenotype in mice, partially effective in rescuing the cardiac outflow tract phenotype in hypomorphic mutants, and ineffective in null mutants. We found an interaction of p53 and Tbx1 in regulating the gene *Gbx2.* Both Tbx1 and p53 occupy a genetic element of the *Gbx2* gene, the expression of which is reduced by *Tbx1* heterozygosity and rescued in compound $Tbx1^{+/-};Trp53^{+/-}$ mutant embryos. Therefore, *Gbx2* is a shared target, and the rescue of its expression in double mutants could explain phenotypic rescue. *Gbx2* and *Tbx1* are coexpressed in the pharyngeal surface ectoderm and in the pharyngeal endoderm (17), tissues that have been linked to the fourth PAA phenotype (17, 27, 28). In addition, *Gbx2* is required for PAA and OFT development (16). We found that p53 regulates positively the enrichment of Ezh2 and H3K27me3 at the genetic element occupied by Tbx1 and p53. These data support the hypothesis that suppression of p53 reduces repressive marks on the *Gbx2* gene and thereby "facilitates" its regulation by Tbx1. This rescue mechanism requires the presence of the Tbx1 protein, thus explaining why p53 suppression has no effect on the null *Tbx1* phenotype.

The enhancement of cell proliferation in the SHF of $Tbx1^{-/neo2}$; $Trp53^{+/-}$ embryos, compared with $Tbx1^{-/neo2}$ embryos, could contribute to the improvement of the OFT phenotype. Indeed, reduced cell proliferation in the SHF has been associated with OFT abnormalities (5, 8, 29). In contrast, it is unlikely that rescue may be due to the antiapoptotic effects of loss of p53 because abnormal apoptosis is not part of the *Tbx1* mutant cardiovascular phenotype (17, 30) (Fig. S1 *C* and *D*).

In view of the complexities of p53 functions in the context of embryonic development and cell differentiation (31–34), it is possible that *Gbx2* is not the only player in phenotypic rescue. Nevertheless, our data about the *Gbx2* gene illustrate an intriguing mechanism of interaction that might function also on other target genes yet to be identified. In addition, recent human genetics data have implicated the p53 pathway in a population of patients affected by Tetralogy of Fallot, a cardiac outflow tract abnormality (35), thus further suggesting that this pathway has relevance for cardiovascular development. Last but not least, our

data provide a proof of concept that the *Tbx1* mutant phenotype can be significantly ameliorated using pharmacological approaches, thus encouraging further studies into the functional mechanisms and interactions of *Tbx1* with the aim of identifying potential drug targets.

Materials and Methods

Details can be found in *SI Materials and Methods*.

Mouse Mutant Lines. We have used lines carrying the alleles *Tbx1*^{lacZ} (here referred to as *Tbx1*$^{-}$) (18), *Tbx1*^{neo2} (36), and *Trp53*$^{-}$ (37). All animal handling and experimentations were performed in accordance with the regulations of the Italian Ministry of Health, in a specific pathogen free (SPF) environment. All mouse lines were maintained in a mixed C57Bl6/129SvEv background.

Quantitative Real-Time PCR, RNA Extraction. Total RNA was isolated using TRIzol (Invitrogen), and RNA from cells or E8.5 embryos was transcribed into cDNA using the High-Capacity cDNA Reverse Transcription kit (Applied Biosystems). Quantitative real-time PCR was performed with FastStart Universal SYBR Green (Roche). Primer sequences are listed in Table S2.

Ink Injection and Histology. Intracardiac ink injection was performed on E10.5 embryos as described (38). For histology and immunohistochemistry, embryos or hearts were embedded in paraffin and cut into 7 or 10 μm sections, respectively. For histology, sections were counter stained with eosin. Immunohistochemistry was carried out using an anti–phospho-Histone H3 (Ser10) antibody and an anti-Isl1 antibody (Developmental Studies Hybridoma Bank).

Coimmunoprecipitation. Coimmunoprecipitation experiments were performed using 5-Azacytidine-DMSO-induced P19CL6 cells after 48 h of induction. Nuclear extracts were immunoprecipitated with an anti-TBX1 antibody (Abcam), with an anti-Ezh2 antibody (BD Biosciences) or with rabbit IgG (Santa Cruz Biotechnology). After immunoprecipitation, samples were extensively washed, resuspended in SDS sample buffer and analyzed by Western blot with an anti-p53 antibody (Santa Cruz Biotechnology) or with an anti-Smarcd1 antibody (BD Bioscience).

Chromatin Immunoprecipitation (ChIP) and Western Blotting. 5-Azacytidine and DMSO induction of differentiation of P19CL6 cells was performed as described (39). Cells were used after 48 h of differentiation. At this stage, cells express *Tbx1*, *Trp53*, and *Gbx2* but do not express cardiac differentiation markers (Fig. S2). For ChIP assay, cells were fixed with 1% formaldehyde Buffer A (Transcription Factor ChIP kit reagent, Diagenode) at room temperature for 10 min. The cross-linking reaction was stopped using 0.125 mol/L glycine at room temperature. Cells were lysed and chromatin was sonicated using S2 Covaris System. Sonicated chromatin (6 μg) was immunoprecipitated with an anti-TBX1 antibody (Abcam), an anti-p53 antibody (Santa Cruz Biotechnology), an anti-H3K27me3 (Millipore), an anti-Ezh2 antibody (BD Biosciences), or Rabbit Control IgG (Abcam) and then incubated at 4 °C overnight with Preblocked protein A/G coated beads. After incubation, immunoprecipitation, samples were extensively washed and reverse cross-linked. DNA was purified and subjected to quantitative PCR amplification.

For ChIP–Western blotting, sonicated chromatin (obtained as described above) was immunoprecipitated with an anti-TBX1 antibody, an anti-p53 antibody, or Control Rabbit IgG; all antibodies were conjugated with Dynabeads Protein G (Novex by Life Technologies). Samples were extensively washed, and DNA–protein complexes were eluted, reverse cross-linked, and subjected to Western blot analysis.

ACKNOWLEDGMENTS. We thank Drs. F. Gabriella Fulcoli for help with biochemical experiments, Claudia Angelini for help with statistical analyses, and Elizabeth Illingworth for critical reading of the manuscript. We acknowledge the support of the Institute of Genetics and Biophysics core facilities Integrated Microscopy, Mouse Transgenics and Flow cytometry. This work was funded in part by Italian Telethon Foundation Grant GGP11029 and Italian Ministry of Research Grant PON01_02342, and FareBio (to A.B.).

1. Papangeli I, Scambler P (2013) The 22q11 deletion: DiGeorge and velocardiofacial syndromes and the role of TBX1. *Wiley Interdiscip Rev Dev Biol* 2(3):393–403.
2. Yagi H, et al. (2003) Role of TBX1 in human del22q11.2 syndrome. *Lancet* 362(9393): 1366–1373.
3. Paylor R, et al. (2006) Tbx1 haploinsufficiency is linked to behavioral disorders in mice and humans: Implications for 22q11 deletion syndrome. *Proc Natl Acad Sci USA* 103(20):7729–7734.
4. Chen L, Fulcoli FG, Tang S, Baldini A (2009) Tbx1 regulates proliferation and differentiation of multipotent heart progenitors. *Circ Res* 105(9):842–851.
5. Vincent SD, Buckingham ME (2010) How to make a heart: The origin and regulation of cardiac progenitor cells. *Curr Top Dev Biol* 90:1–41.
6. Watanabe Y, et al. (2012) Fibroblast growth factor 10 gene regulation in the second heart field by Tbx1, Nkx2-5, and Islet1 reveals a genetic switch for down-regulation in the myocardium. *Proc Natl Acad Sci USA* 109(45):18273–18280.
7. Xu H, et al. (2007) Tbx1 regulates population, proliferation and cell fate determination of otic epithelial cells. *Dev Biol* 302(2):670–682.
8. Xu H, et al. (2004) Tbx1 has a dual role in the morphogenesis of the cardiac outflow tract. *Development* 131(13):3217–3227.
9. Cao H, et al. (2010) Tbx1 regulates progenitor cell proliferation in the dental epithelium by modulating Pitx2 activation of p21. *Dev Biol* 347(2):289–300.
10. Chen T, et al. (2012) An RNA interference screen uncovers a new molecule in stem cell self-renewal and long-term regeneration. *Nature* 485(7396):104–108.
11. Jain AK, et al. (2012) p53 regulates cell cycle and microRNAs to promote differentiation of human embryonic stem cells. *PLoS Biol* 10(2):e1001268.
12. Lin T, et al. (2005) p53 induces differentiation of mouse embryonic stem cells by suppressing Nanog expression. *Nat Cell Biol* 7(2):165–171.
13. Meletis K, et al. (2006) p53 suppresses the self-renewal of adult neural stem cells. *Development* 133(2):363–369.
14. Tapia N, Schöler HR (2010) p53 connects tumorigenesis and reprogramming to pluripotency. *J Exp Med* 207(10):2045–2048.
15. Menendez S, Camus S, Izpisua Belmonte JC (2010) p53: Guardian of reprogramming. *Cell Cycle* 9(19):3887–3891.
16. Byrd NA, Meyers EN (2005) Loss of Gbx2 results in neural crest cell patterning and pharyngeal arch artery defects in the mouse embryo. *Dev Biol* 284(1):233–245.
17. Calmont A, et al. (2009) Tbx1 controls cardiac neural crest cell migration during arch artery development by regulating Gbx2 expression in the pharyngeal ectoderm. *Development* 136(18):3173–3183.
18. Lindsay EA, et al. (2001) Tbx1 haploinsufficieny in the DiGeorge syndrome region causes aortic arch defects in mice. *Nature* 410(6824):97–101.
19. Merscher S, et al. (2001) TBX1 is responsible for cardiovascular defects in velo-cardio-facial/DiGeorge syndrome. *Cell* 104(4):619–629.
20. Jerome LA, Papaioannou VE (2001) DiGeorge syndrome phenotype in mice mutant for the T-box gene, Tbx1. *Nat Genet* 27(3):286–291.
21. Komarov PG, et al. (1999) A chemical inhibitor of p53 that protects mice from the side effects of cancer therapy. *Science* 285(5434):1733–1737.
22. Xu H, Cerrato F, Baldini A (2005) Timed mutation and cell-fate mapping reveal reiterated roles of Tbx1 during embryogenesis, and a crucial function during segmentation of the pharyngeal system via regulation of endoderm expansion. *Development* 132(19):4387–4395.
23. Zhang Z, Baldini A (2008) In vivo response to high-resolution variation of Tbx1 mRNA dosage. *Hum Mol Genet* 17(1):150–157.
24. Papangeli I, Scambler PJ (2013) Tbx1 genetically interacts with the transforming growth factor-β/bone morphogenetic protein inhibitor Smad7 during great vessel remodeling. *Circ Res* 112(1):90–102.
25. Chen L, et al. (2012) Transcriptional control in cardiac progenitors: Tbx1 interacts with the BAF chromatin remodeling complex and regulates Wnt5a. *PLoS Genet* 8(3):e1002571.
26. Yang Y, et al. (2013) Polycomb group protein PHF1 regulates p53-dependent cell growth arrest and apoptosis. *J Biol Chem* 288(1):529–539.
27. Zhang Z, et al. (2005) Tbx1 expression in pharyngeal epithelia is necessary for pharyngeal arch artery development. *Development* 132(23):5307–5315.
28. Randall V, et al. (2009) Great vessel development requires biallelic expression of Chd7 and Tbx1 in pharyngeal ectoderm in mice. *J Clin Invest* 119(11):3301–3310.
29. Prall OW, et al. (2007) An Nkx2-5/Bmp2/Smad1 negative feedback loop controls heart progenitor specification and proliferation. *Cell* 128(5):947–959.
30. Vitelli F, Morishima M, Taddei I, Lindsay EA, Baldini A (2002) Tbx1 mutation causes multiple cardiovascular defects and disrupts neural crest and cranial nerve migratory pathways. *Hum Mol Genet* 11(8):915–922.
31. Rivlin N, Koifman G, Rotter V (2014) p53 orchestrates between normal differentiation and cancer. *Semin Cancer Biol*, 10.1016/j.semcancer.2013.12.006.
32. Danilova N, Sakamoto KM, Lin S (2008) p53 family in development. *Mech Dev* 125(11-12):919–931.
33. Armstrong JF, Kaufman MH, Harrison DJ, Clarke AR (1995) High-frequency developmental abnormalities in p53-deficient mice. *Curr Biol* 5(8):931–936.
34. Sah VP, et al. (1995) A subset of p53-deficient embryos exhibit exencephaly. *Nat Genet* 10(2):175–180.
35. Grunert M, et al. (2014) Rare and private variations in neural crest, apoptosis and sarcomere genes define the polygenic background of isolated Tetralogy of Fallot. *Hum Mol Genet* 23(12):3115–3128.
36. Zhang Z, Huynh T, Baldini A (2006) Mesodermal expression of Tbx1 is necessary and sufficient for pharyngeal arch and cardiac outflow tract development. *Development* 133(18):3587–3595.
37. Jacks T, et al. (1994) Tumor spectrum analysis in p53-mutant mice. *Curr Biol* 4(1):1–7.
38. Lindsay EA, et al. (1999) Congenital heart disease in mice deficient for the DiGeorge syndrome region. *Nature* 401(6751):379–383.
39. Mueller I, Kobayashi R, Nakajima T, Ishii M, Ogawa K (2010) Effective and steady differentiation of a clonal derivative of P19CL6 embryonal carcinoma cell line into beating cardiomyocytes. *J Biomed Biotechnol* 2010:380561.